symmetry

Article

Quasi-Synchronization and Quasi-Uniform Synchronization of Caputo Fractional Variable-Parameter Neural Networks with Probabilistic Time-Varying Delays

Renyu Ye, Chen Wang, Axiu Shu and Hai Zhang *

School of Mathematics and Physics, Anqing Normal University, Anqing 246133, China; yereny@aqnu.edu.cn (R.Y.); chenwang218@aqnu.edu.cn (C.W.); shuaxiu@aqnu.edu.cn (A.S.)
* Correspondence: zhanghai@aqnu.edu.cn

Abstract: Owing to the symmetry between drive–response systems, the discussions of synchronization performance are greatly significant while exploring the dynamics of neural network systems. This paper investigates the quasi-synchronization (QS) and quasi-uniform synchronization (QUS) issues between the drive–response systems on fractional-order variable-parameter neural networks (VPNNs) including probabilistic time-varying delays. The effects of system parameters, probability distributions and the order on QS and QUS are considered. By applying the Lyapunov–Krasovskii functional approach, Hölder's inequality and Jensen's inequality, the synchronization criteria of fractional-order VPNNs under controller designs with constant gain coefficients and time-varying gain coefficients are derived. The obtained criteria are related to the probability distributions and the order of the Caputo derivative, which can greatly avoid the situation in which the upper bound of an interval with time delay is too large yet the probability of occurrence is very small, and information such as the size of time delay and probability of occurrence is fully considered. Finally, two examples are presented to further confirm the effectiveness of the algebraic criteria under different probability distributions.

Keywords: Caputo derivative; variable parameter; probabilistic time-varying delays; quasi-synchronization; quasi-uniform synchronization

Citation: Ye, R.; Wang, C.; Shu, A.; Zhang, H. Quasi-Synchronization and Quasi-Uniform Synchronization of Caputo Fractional Variable-Parameter Neural Networks with Probabilistic Time-Varying Delays. *Symmetry* **2022**, *14*, 1035. https://doi.org/10.3390/sym14051035

Academic Editors: Garik Petrosyan and Alexander Zaslavski

Received: 19 April 2022
Accepted: 14 May 2022
Published: 18 May 2022

1. Introduction

Neural networks (NNs) form different network models according to different connection modes of neurons, which have powerful functions and characteristics, including nonlinear approximation, self-learning and adaptive ability [1–5]. The fractional derivative has a nonlocal and weak singular kernel, which provides a wonderful tool to present the memory and genetic characteristics of many phenomena and processes. Therefore, the combination of NNs and fractional calculus is a very meaningful research topic. Along with Arena [6] establishing fractional-order cellular NNs with fractional-order cells, fractional-order NNs have become a popular field among scholars [7–12].

As far as we know, most works relative to fractional-order NNs involve constant coefficients, while many factors affect the speed and communication between neurons, and the transmission speed and the weight of the connection matrix usually change with time. Thus, the variable-parameter fractional-order NN model is an excellent tool to precisely describe the information transmission process between neurons. Recently, Wang et al. [13] utilized differential inclusion theory to discuss the finite-time synchronization of fractional-order NNs with time-varying parameters.

Actually, time delays are inescapable because signal processing and transmission are not finished immediately. The discussions of delayed NNs of fractional order have obtained extensive attention recently [14–21]. Utilizing the Gronwall–Bellman integral inequality, Pratap et al. [15] investigated the synchronization issue of fractional competitive delayed NNs based on a finite-time output feedback controller. Cao et al. [19] established the almost periodicity criteria for fractional-order delayed NNs including reaction-diffusion terms and impulsive perturbations. Zhang et al. [20] discussed synchronization stability for Riemann–Liouville coupled NNs with delays by the LMI method. As far as we know, although some delay values are very large in applications such as high-performance aircrafts, they hardly happen. If only the change of delay is simply considered, the results may be conservative. Up until now, there has not been enough discussion about fractional NNs with probabilistic time-varying delays in the existing literature. Therefore, it is challenging and meaningful to explore the dynamics of fractional NNs with probabilistic time-varying delays.

Synchronization has been favored by researchers in information security and confidential communication over recent years. However, the synchronization phenomenon is two-sided, which is both beneficial and harmful. Therefore, how to amplify its advantages, increase favorable synchronization, reduce harmful synchronization and make synchronization better serve the real world is the original intention of scholars to study the synchronization phenomenon. Hitherto, synchronization methods can be roughly divided into several types [22–33], such as quasi-synchronization [22], cluster synchronization [23], projective synchronization [24–26], lag synchronization [27], Mittag–Leffler synchronization [28–30], finite-time synchronization [31], quasi-uniform synchronization [32,33] and so on. In [24], Zhang et al. chose the appropriate adaptive controllers to obtain the projective synchronization criteria for fractional-order delayed NNs, where the probability time-varying delays and variable parameters had not been considered.

As we have yet seen, the results of QS and QUS for fractional-order VPNNs including probabilistic time-varying delays in the existing literature have not been found. In this paper, by means of the Lyapunov functional technique and the Volterra expansion method, the algebraic criteria for the QS and QUS of fractional-order VPNNs with probabilistic time-varying delays are derived by designing the controllers about the constant gain coefficient and the control gain time-dependent coefficient. In addition, inspired by the simulation method in [34,35], we improve the numerical simulation based on the predictor-corrector scheme of fractional delayed differential equations. Thus, the appropriate sampling step can be selected to ensure the stability and acceptable quality of the considered systems. The highlights and innovations of this paper are summarized below:

- The effects of the system parameters, the probability distributions and the order of Caputo derivative on QS and QUS are discussed.
- Different from the exploration method of the system in [7,17,20,21], in this paper, Volterra integral expansion, Hölder's inequality and Jensen's inequality are applied to establish two synchronization criteria between the drive–response systems.
- The presented results are related to the algebraic inequalities containing the probability distributions and the order of the Caputo derivative, which deeply reveal the factors affecting synchronization performance.
- Two examples are given to further substantiate the validity and applicability of the criteria under the different probability distributions.

2. Preliminaries

This part mainly recalls some fundamental definitions, and the fractional-order VPNN system is proposed.

Definition 1 ([36]). *For any $\mu > 0$, the Riemann–Liouville-type fractional integral is defined as*

$$D^{-\mu}v(t) = \frac{1}{\Gamma(\mu)}\int_{t_0}^{t}(t-s)^{\mu-1}v(s)ds.$$

Definition 2 ([36]). *For any $\mu \in (n-1, n)$, the Caputo-type fractional derivative is defined as*

$$D^{\mu}v(t) = \frac{1}{\Gamma(n-\mu)}\int_{t_0}^{t}\frac{v^{(n)}(s)}{(t-s)^{\mu-n+1}}ds,\ t \geqslant t_0.$$

Definition 3 ([22,33]). *For any positive number γ, if there exists a constant $T \geqslant 0$ such that $\|e(t)\| < \gamma$ holds, then the error system in (3) can achieve QS. If there exists a constant $\delta \in (0, \gamma)$ such that $\|e(t)\| < \gamma$ holds when $\|e(0)\| < \delta$, then the error system in (3) can realize QUS.*

Lemma 1 ([22]). *Suppose $x(\cdot)$ is a continuous function in the interval $[0, +\infty)$. If*

$$D^{\varepsilon} x(t) \leqslant -\alpha x(t) + \beta,$$

then

$$x(t) \leqslant \Big[x(0) - \frac{\beta}{\alpha}\Big] E_{\varepsilon}\big(-\alpha t^{\beta}\big) + \frac{\beta}{\alpha}, \;\; \varepsilon \in (0,1),\; \alpha \neq 0,$$

where $x(0)$ is the initial value.

Lemma 2 ([32]). *Suppose $x(\cdot), y(\cdot)$ and $z(\cdot)$ are continuous functions in the interval $[0, +\infty)$. If the function $z(t)$ satisfies $z(t) \leqslant x(t) + \int_0^t y(\theta) z(\theta) d\theta$, then*

$$z(t) \leqslant x(t) \exp\Big(\int_0^t y(\theta) d\theta\Big), \;\; t \in [0, +\infty),$$

where $x(t)$ is nondecreasing and $y(t) > 0$.

In this paper, the following drive–response systems (1) and (2) of fractional-order VPNNs are considered:

$$D^{\mu} v_k(t) = -a_k(t) v_k(t) + \sum_{g=1}^{M} b_{kg}(t) y_g\big(v_g(t)\big) + \sum_{g=1}^{M} c_{kg}(t) y_g\big(v_g(t - \tau(t))\big) + J_k, \tag{1}$$

$$D^{\mu} v'_k(t) = -a_k(t) v'_k(t) + \sum_{g=1}^{M} b_{kg}(t) y_g\big(v'_g(t)\big) + \sum_{g=1}^{M} c_{kg}(t) y_g\big(v'_g(t - \tau(t))\big) + J_k + U_k(t), \tag{2}$$

where $0 < \mu < 1$, $v_k(t)$ and $v'_k(t)$ represent the state variables, D represents the fractional Caputo-type operator, $a_k(t)$ denotes the self-regulating parameter, $b_{kg}(t), c_{kg}(t)$ and $d_{kg}(t)$ signify the connection weights, $y(\cdot)$ stands for the continuous activation function, $\tau(t)$ is the time-varying delay, J_k is the external input and $U_k(\cdot)$ denotes the controller.

Remark 1. *In this article, the QS and QUS of the fractional-order systems (1) and (2) with time-varying parameters are discussed. The value of self-regulating parameter $a_k(t)$ and connection weights $b_k(t)$ and $c_k(t)$ of the system are expressions of time t. As far as we know, most fractional-order NNs' parameters are fixed constants, yet that is actually not the case. Therefore, it is worth exploring the dynamical behaviors of network systems with time-varying parameters.*

Now, we describe the error system of Systems (1) and (2) by

$$\begin{aligned} D^{\mu} e_k(t) =& -a_k(t) e_k(t) + \sum_{g=1}^{M} b_{kg}(t) [y_g\big(v'_g(t)\big) - y_g\big(v_g(t)\big)] \\ &+ \sum_{g=1}^{M} c_{kg}(t) [y_g\big(v'_g(t - \tau(t))\big) - y_g\big(v_g(t - \tau(t))\big)] + U_k(t), \end{aligned} \tag{3}$$

where $e_k(t) = v'_k(t) - v_k(t)$.

In order to conveniently derive the main results, we divide the time-varying delay $\tau(t)$ into two parts $\tau_1(t)$ and $\tau_2(t)$. The following hypothetical conditions are satisfied throughout this paper.

Assumption 1. *$\tau_1(t)$ and $\tau_2(t)$ are bounded with $0 \leqslant \tau_1 \leqslant \tau_1(t) \leqslant \tau_2 \leqslant \tau_2(t) \leqslant \tau_3$. When $t \in [\tau_1, \tau_2]$, the stochastic variable is $\varepsilon(t) = 1$; when $t \in (\tau_2, \tau_3]$, the stochastic variable is $\varepsilon(t) = 0$. Moreover, $\tau_1(t)$ and $\tau_2(t)$ are derivable, $\theta_1 \leqslant \dot{\tau}_1(t) \leqslant \theta_2, \theta_3 \leqslant \dot{\tau}_2(t) \leqslant \theta_4$ and*

$$\tau_4 = \max\left\{ \sup_{s\in[0,T]} \frac{1}{|1-\dot{\tau}_1(s)|}, \sup_{s\in[0,T]} \frac{1}{|1-\dot{\tau}_2(s)|} \right\}. \tag{4}$$

Assumption 2. *If $t \in [\tau_1, \tau_3]$, then the probability distributions are given by*

$$\begin{cases} \text{prob}\{\varepsilon(t)=1\} = \mathbb{E}\{\varepsilon(t)\} = \varepsilon_0, \ \tau_1 \leqslant \tau(t) \leqslant \tau_2, \\ \text{prob}\{\varepsilon(t)=0\} = 1 - \mathbb{E}\{\varepsilon(t)\} = 1-\varepsilon_0, \ \tau_2 < \tau(t) \leqslant \tau_3, \end{cases} \tag{5}$$

where $\mathbb{E}$ signifies the mathematical expectation.

Assumption 3. *For any activation function $y(\cdot)$, the following inequality holds:*

$$\left|y_g(v_1) - y_g(v_2)\right| \leqslant l_g\left|v_1 - v_2\right|, \tag{6}$$

where l_g is the Lipschitz constant.

From Assumption 1, System (3) is equivalent to

$$\begin{aligned} D^{\mu}e_k(t) =& -a_k(t)e_k(t) + \sum_{g=1}^{M} b_{kg}(t)[y_g(v_g'(t)) - y_g(v_g(t))] \\ &+ \varepsilon(t)\sum_{g=1}^{M} c_{kg}(t)[y_g(v_g'(t-\tau_1(t))) - y_g(v_g(t-\tau_1(t)))] \\ &+ (1-\varepsilon(t))\sum_{g=1}^{M} c_{kg}(t)[y_g(v_g'(t-\tau_2(t))) - y_g(v_g(t-\tau_2(t)))] + U_k(t). \end{aligned} \tag{7}$$

Remark 2. *Compared with the systems in [3,7,9,12,15,19], a novel network model is extended including the probability distributions of time-varying delays in the different intervals. Although the upper bound of some time delays may be too large, it will hardly happen. The processing method is to segment the time delay and describe the probability of different intervals by introducing a random variable subject to the Bernoulli distribution. By comparing Systems (3) and (7), it can be seen that when $\varepsilon(t) = 0$, System (7) can be rewritten in the form of System (3).*

Remark 3. *This article discusses the case that the time-varying delay is divided into two parts based on the probability distributions in Assumption 2. In practical applications, it can be divided into multiple parts according to the probability distributions of each part.*

3. Main Results

In this section, the synchronization criteria of the QS and QUS of fractional-order VPNNs under controller designs with constant gain coefficients and time-varying gain coefficients are derived by applying the Lyapunov–Krasovskii functional approach, Hölder's inequality and Jensen's inequality.

The controller $U_k(\cdot)$ can be configured as

$$U_k(t) = -w_k e_k(t) + \frac{r_k e_k(t)}{\|e(t)\|^4 + r_k^4}, \tag{8}$$

where $w_k, r_k \in \mathbb{R}$ are constant gain coefficients.

Theorem 1. *Under Assumptions 1–3, if there exist positive constants $\theta_1, \theta_2 > 1$ such that*

$$\Psi_1 - \theta_1\Psi_2 - \theta_2\Psi_3 > 0, \tag{9}$$

then Systems (1) *and* (2) *can reach QS, where*

$$\Psi_1 = \min_{k\in M}\Big\{2w_k + 2a_k(t) - \sum_{g=1}^{M} l_g|b_{kg}(t)| - \sum_{g=1}^{M} l_k|b_{gk}(t)| - \sum_{g=1}^{M} l_g|c_{kg}(t)|\Big\},$$
$$\Psi_2 = \max_{k\in M}\Big\{\varepsilon_0 \sum_{g=1}^{M} l_k|c_{gk}(t)|\Big\},$$
$$\Psi_3 = \max_{k\in M}\Big\{(1-\varepsilon_0)\sum_{g=1}^{M} l_k|c_{gk}(t)|\Big\}.$$

Proof. We take the function $V(\cdot)$ below:

$$V(t) = \sum_{k=1}^{M} e_k^2(t). \tag{10}$$

Calculating the μ-order derivative of $V(t)$ and based on Assumption 3, we have

$$\begin{aligned}
D^{\mu}V(t) \leqslant{}& \sum_{k=1}^{M} 2e_k(t)D^{\mu}e_k(t)\\
={}& \sum_{k=1}^{M} 2e_k(t)\Big\{-a_k(t)e_k(t) + \sum_{g=1}^{M} b_{kg}(t)[y_g(v'_g(t)) - y_g(v_g(t))]\\
&+ \varepsilon(t)\sum_{g=1}^{M} c_{kg}(t)[y_g(v'_g(t-\tau_1(t))) - y_g(v_g(t-\tau_1(t)))]\\
&+ (1-\varepsilon(t))\sum_{g=1}^{M} c_{kg}(t)[y_g(v'_g(t-\tau_2(t))) - y_g(v_g(t-\tau_2(t)))]\Big\} + 2e_k(t)U_k(t)\\
\leqslant{}& \sum_{k=1}^{M} 2e_k(t)\Big\{-a_k(t)e_k(t) + \sum_{g=1}^{M} b_{kg}(t)l_g e_g(t) + \varepsilon(t)\sum_{g=1}^{M} c_{kg}(t)l_g e_g(t-\tau_1(t))\\
&+ (1-\varepsilon(t))\sum_{g=1}^{M} c_{kg}(t)l_g e_g(t-\tau_2(t))\Big\} + \sum_{k=1}^{M} 2e_k(t)\big(-w_k e_k(t) + \frac{r_k e_k(t)}{\|e(t)\|^4 + r_k^4}\big)\\
\leqslant{}& \sum_{k=1}^{M}\big[-2w_k - 2a_k(t) + \sum_{g=1}^{M} l_g|b_{kg}(t)| + \sum_{g=1}^{M} l_k|b_{gk}(t)| + \sum_{g=1}^{M} l_g|c_{kg}(t)|\big]e_k^2(t)\\
&+ \varepsilon(t)\sum_{k=1}^{M}\sum_{g=1}^{M} l_k|c_{gk}(t)|e_k^2(t-\tau_1(t)) + (1-\varepsilon(t))\sum_{k=1}^{M}\sum_{g=1}^{M} l_k|c_{gk}(t)|e_k^2(t-\tau_2(t))\\
&+ 2\frac{r\|e(t)\|}{\|e(t)\|^4 + r^4}.
\end{aligned} \tag{11}$$

According to Assumption 2, we obtain

$$\begin{aligned}
\mathbb{E}\{D^{\mu}V(t)\} \leqslant{}& \mathbb{E}\Big\{\sum_{k=1}^{M}\big[-2w_k - 2a_k(t) + \sum_{g=1}^{M} l_g|b_{kg}(t)| + \sum_{g=1}^{M} l_k|b_{gk}(t)| + \sum_{g=1}^{M} l_g|c_{kg}(t)|\big]e_k^2(t)\\
&+ \varepsilon_0\sum_{k=1}^{M}\sum_{g=1}^{M} l_k|c_{gk}(t)|e_k^2(t-\tau_1(t)) + (1-\varepsilon_0)\sum_{k=1}^{M}\sum_{g=1}^{M} l_k|c_{gk}(t)|e_k^2(t-\tau_2(t))\\
&+ 2\frac{r\|e(t)\|}{\|e(t)\|^4 + r^4}\Big\}\\
\leqslant{}& \mathbb{E}\big\{-\Psi_1 V(t) + \Psi_2 V(t-\tau_1(t)) + \Psi_3 V(t-\tau_2(t)) + 2\frac{r\|e(t)\|}{\|e(t)\|^4 + r^4}\big\}\\
\leqslant{}& \mathbb{E}\big\{-(\Psi_1 - \theta_1\Psi_2 - \theta_2\Psi_3)V(t) + 2\frac{r\|e(t)\|}{\|e(t)\|^4 + r^4}\big\}.
\end{aligned} \tag{12}$$

With the help of the significant inequality $2(x^4+y^4) \geqslant xy(x+y)^2$ for $x, y \in \mathbb{R}$, we can obtain

$$\begin{aligned}\mathbb{E}\{D^{\mu}V(t)\} \leqslant& \mathbb{E}\Big\{-(\Psi_1-\theta_1\Psi_2-\theta_2\Psi_3)V(t)+\frac{4}{(\|e(t)\|+r)^2}\Big\}\\ \leqslant& \mathbb{E}\Big\{-(\Psi_1-\theta_1\Psi_2-\theta_2\Psi_3)V(t)+\frac{4}{r^2}\Big\}.\end{aligned} \tag{13}$$

From Lemma 1, one has

$$\begin{aligned}\mathbb{E}\{V(t)\} \leqslant& \mathbb{E}\Big\{\Big[V(0)-\frac{4}{r^2(\Psi_1-\theta_1\Psi_2-\theta_2\Psi_3)}\Big]E_{\mu}(-(\Psi_1-\theta_1\Psi_2-\theta_2\Psi_3)t^{\mu})\\ &+\frac{4}{r^2(\Psi_1-\theta_1\Psi_2-\theta_2\Psi_3)}\Big\}.\end{aligned} \tag{14}$$

Namely,

$$\begin{aligned}\mathbb{E}\{\|e(t)\|\} \leqslant& \mathbb{E}\Bigg\{\Big[(\|e(0)\|-\frac{4}{r^2(\Psi_1-\theta_1\Psi_2-\theta_2\Psi_3)})E_{\mu}\Big(-(\Psi_1-\theta_1\Psi_2-\theta_2\Psi_3)t^{\mu}\Big)\\ &+\frac{4}{r^2(\Psi_1-\theta_1\Psi_2-\theta_2\Psi_3)}\Big]^{\frac{1}{2}}\Bigg\}.\end{aligned} \tag{15}$$

Note that if $E_{\mu}(\alpha t^{\mu})$ is monotonically nonincreasing and $E_{\mu}(\alpha t^{\mu}) \in (0,1)$ for $\alpha \leqslant 0$, then both sides can take the limit at the same time:

$$\lim_{t\to+\infty}\mathbb{E}\{\|e(t)\|\} \leqslant \frac{2}{\sqrt{r^2(\Psi_1-\theta_1\Psi_2-\theta_2\Psi_3)}}. \tag{16}$$

Thus, Systems (1) and (2) achieve QS. □

In order to discuss the QUS of System (6), a linear feedback controller with variable control gain is designed as

$$U_k(t) = -\zeta_k(t)e_k(t). \tag{17}$$

Remark 4. *In contrast to the controller (8) in Theorem 1, the control gain of the controller in (17) by QUS is time-dependent in Theorem 2. The advantage of this kind of design is that the control coefficient can be changed automatically according to the change of time t so that the controller can be better applied to the actual situation.*

Theorem 2. *If there exists a positive number $M = \max\Big\{A(t), B(t), C(t), \zeta(t)\Big\}$ such that*

$$\Big[1+\varepsilon_0 e^{t-\tau_1}H_1H_2+(1-\varepsilon_0)e^{t-\tau_2}H_1H_2\Big]H_1M\Big[(2+L)e^t+\varepsilon_0\tau_4Le^{t-\tau_1}+(1-\varepsilon_0)\tau_4Le^{t-\tau_2}\Big](1-e^{-t}) \leqslant \frac{\gamma}{\delta}, \tag{18}$$

then Systems (1) and (2) can achieve QUS, where $\alpha, \beta > 0$, $\frac{1}{\alpha}+\frac{1}{\beta}=1$ and

$$H_1 = \frac{1}{\Gamma(\mu)}\Big[\frac{\Gamma\big(\alpha(\mu-1)+1\big)}{\alpha^{\alpha\mu-\alpha+1}}\Big]^{\frac{1}{\alpha}},\ H_2 = ML\Big[\frac{(e^{\beta\tau_2}-1)\tau_4}{\beta}\Big]^{\frac{1}{\beta}}.$$

Proof. System (6) can be rewritten as

$$
\begin{aligned}
e_k(t) =& e_k(0) + \int_0^t \frac{(t-s)^{\mu-1}}{\Gamma(\mu)} \bigg\{ - a_k(s)e_k(s) + \sum_{g=1}^{M} b_{kg}(s)[y_g(v'_g(s)) - y_g(v_g(s))] \\
&+ \varepsilon(s) \sum_{g=1}^{M} c_{kg}(s)[y_g(v'_g(s-\tau_1(s))) - y_g(v_g(s-\tau_1(s)))] \\
&+ (1-\varepsilon(s)) \sum_{g=1}^{M} c_{kg}(s)[y_g(v'_g(s-\tau_2(s))) - y_g(v_g(s-\tau_2(s)))] - \zeta_k(s)e_k(s) \bigg\} ds \\
\leqslant & e_k(0) + \int_0^t \frac{(t-s)^{\mu-1}}{\Gamma(\mu)} \bigg\{ - a_k(s)e_k(s) + \sum_{g=1}^{M} b_{kg}(s) l_g e_g(s) + \varepsilon(s) \sum_{g=1}^{M} c_{kg}(s) l_g e_g(s \\
&- \tau_1(s)) + (1-\varepsilon(s)) \sum_{g=1}^{M} c_{kg}(s) l_g e_g(s-\tau_2(s)) - \zeta_k(s)e_k(s) \bigg\} ds.
\end{aligned} \tag{19}
$$

We can write (19) in vector form and take norms on both sides of the inequality at the same time:

$$
\begin{aligned}
\|e(t)\| \leqslant & \|e(0)\| + \int_0^t \frac{(t-s)^{\mu-1}}{\Gamma(\mu)} \big(\|A(s)\| + \|B(s)\|L + \|\zeta(s)\|\big)\|e(s)\| ds \\
&+ \int_0^t \frac{(t-s)^{\mu-1}}{\Gamma(\mu)} \|\varepsilon(s)\| \|C(s)\| L \|e(s-\tau_1(s)\| ds \\
&+ \int_0^t \frac{(t-s)^{\mu-1}}{\Gamma(\mu)} \|1-\varepsilon(s)\| \|C(s)\| L \|e(s-\tau_2(s)\| ds.
\end{aligned} \tag{20}
$$

From Assumption 2 and Hölder's inequality, we have

$$
\begin{aligned}
\mathbb{E}\{\|e(t)\|\} \leqslant & \mathbb{E}\bigg\{ \|e(0)\| + \int_0^t \frac{(t-s)^{\mu-1}}{\Gamma(\mu)} \big(\|A(s)\| + \|B(s)\|L + \|\zeta(s)\|\big)\|e(s)\| ds \\
&+ \int_0^t \frac{(t-s)^{\mu-1}}{\Gamma(\mu)} \varepsilon_0 \|C(s)\| L \|e(s-\tau_1(s)\| ds \\
&+ \int_0^t \frac{(t-s)^{\mu-1}}{\Gamma(\mu)} (1-\varepsilon_0) \|C(s)\| L \|e(s-\tau_2(s)\| ds \bigg\} \\
\leqslant & \mathbb{E}\bigg\{ \|e(0)\| + \frac{2M+ML}{\Gamma(\mu)} \int_0^t (t-s)^{\mu-1} e^s e^{-s} \|e(s)\| ds \\
&+ \frac{\varepsilon_0 ML}{\Gamma(\mu)} \int_0^t (t-s)^{\mu-1} e^s e^{-s} \|e(s-\tau_1(s)\| ds \\
&+ \frac{(1-\varepsilon_0)ML}{\Gamma(\mu)} \int_0^t (t-s)^{\mu-1} e^s e^{-s} \|e(s-\tau_2(s)\| ds \bigg\} \\
\leqslant & \mathbb{E}\bigg\{ \|e(0)\| + \frac{2M+ML}{\Gamma(\mu)} \Big[\int_0^t (t-s)^{\alpha(\mu-1)} e^{\alpha s} ds \Big]^{\frac{1}{\alpha}} \Big[\int_0^t e^{-\beta s} \|e(s)\|^{\beta} ds \Big]^{\frac{1}{\beta}} \\
&+ \frac{\varepsilon_0 ML}{\Gamma(\mu)} \Big[\int_0^t (t-s)^{\alpha(\mu-1)} e^{\alpha s} ds \Big]^{\frac{1}{\alpha}} \Big[\int_0^t e^{-\beta s} \|e(s-\tau_1(s)\|^{\beta} ds \Big]^{\frac{1}{\beta}} \\
&+ \frac{(1-\varepsilon_0)ML}{\Gamma(\mu)} \Big[\int_0^t (t-s)^{\alpha(\mu-1)} e^{\alpha s} ds \Big]^{\frac{1}{\alpha}} \Big[\int_0^t e^{-\beta s} \|e(s-\tau_2(s)\|^{\beta} ds \Big]^{\frac{1}{\beta}} \bigg\}.
\end{aligned} \tag{21}
$$

Since

$$\begin{aligned}\int_0^t (t-s)^{\alpha(\mu-1)} e^{\alpha s} ds = \int_0^t \varpi^{\alpha(\mu-1)} e^{\alpha(1-\varpi)} d\varpi = e^{\alpha t} \int_0^t \varpi^{\alpha\mu-1} e^{-\alpha\varpi} d\varpi \\ = \frac{e^{\alpha t}}{\alpha^{\alpha\mu-\alpha+1}} \int_0^{\alpha t} \kappa^{\alpha(\mu-1)} e^{-\kappa} d\kappa \leqslant \frac{e^{\alpha t}}{\alpha^{\alpha\mu-\alpha+1}} \Gamma\big(\alpha(\mu-1)+1\big),\end{aligned} \tag{22}$$

thus, combining (21) and (22) and using Jensen's inequality, one has

$$\begin{aligned}\mathbb{E}\{\|e(t)\|\} \leqslant & \mathbb{E}\bigg\{ \|e(0)\| + \frac{2M+ML}{\Gamma(\mu)} \left[\frac{e^{\alpha t}\Gamma\big(\alpha(\mu-1)+1\big)}{\alpha^{\alpha\mu-\alpha+1}} \right]^{\frac{1}{\alpha}} \Big[\int_0^t e^{-\beta s} \|e(s)\|^\beta ds \Big]^{\frac{1}{\beta}} \\ & + \frac{\varepsilon_0 ML}{\Gamma(\mu)} \left[\frac{e^{\alpha t}\Gamma\big(\alpha(\mu-1)+1\big)}{\alpha^{\alpha\mu-\alpha+1}} \right]^{\frac{1}{\alpha}} \bigg[\int_0^t e^{-\beta(s-\tau_1(s))} e^{-\beta\tau_1(s)} \\ & \times \frac{\|e(s-\tau_1(s)\|^\beta}{|1-\dot{\tau}_1(s)|} d(s-\tau_1(s)) \bigg]^{\frac{1}{\beta}} + \frac{(1-\varepsilon_0)ML}{\Gamma(\mu)} \left[\frac{e^{\alpha t}\Gamma\big(\alpha(\mu-1)+1\big)}{\alpha^{\alpha\mu-\alpha+1}} \right]^{\frac{1}{\alpha}} \\ & \times \bigg[\int_0^t e^{-\beta(s-\tau_2(s))} e^{-\beta\tau_2(s)} \frac{\|e(s-\tau_2(s)\|^\beta}{|1-\dot{\tau}_2(s)|} d(s-\tau_2(s)) \bigg]^{\frac{1}{\beta}} \bigg\} \\ \leqslant & \mathbb{E}\bigg\{ \|e(0)\| + \frac{2M+ML}{\Gamma(\mu)} \left[\frac{e^{\alpha t}\Gamma\big(\alpha(\mu-1)+1\big)}{\alpha^{\alpha\mu-\alpha+1}} \right]^{\frac{1}{\alpha}} \Big[\int_0^t e^{-\beta s} \|e(s)\|^\beta ds \Big]^{\frac{1}{\beta}} \\ & + \frac{\varepsilon_0 ML}{\Gamma(\mu)} \left[\frac{e^{\alpha t}\Gamma\big(\alpha(\mu-1)+1\big)}{\alpha^{\alpha\mu-\alpha+1}} \right]^{\frac{1}{\alpha}} \Big[\int_{-\tau_2}^0 \tau_4 e^{-\beta s} e^{-\beta\tau_1} \|e(0)\|^\beta ds \\ & + \int_0^t \tau_4 e^{-\beta s} e^{-\beta\tau_1} \|e(s)\|^\beta ds \Big]^{\frac{1}{\beta}} + \frac{(1-\varepsilon_0)ML}{\Gamma(\mu)} \left[\frac{e^{\alpha t}\Gamma\big(\alpha(\mu-1)+1\big)}{\alpha^{\alpha\mu-\alpha+1}} \right]^{\frac{1}{\alpha}} \\ & \times \Big[\int_{-\tau_3}^0 \tau_4 e^{-\beta s} e^{-\beta\tau_2} \|e(0)\|^\beta ds + \int_0^t \tau_4 e^{-\beta s} e^{-\beta\tau_2} \|e(s)\|^\beta ds \Big]^{\frac{1}{\beta}} \bigg\} \\ = & \mathbb{E}\bigg\{ \|e(0)\| + \frac{2M+ML}{\Gamma(\mu)} \left[\frac{e^{\alpha t}\Gamma\big(\alpha(\mu-1)+1\big)}{\alpha^{\alpha\mu-\alpha+1}} \right]^{\frac{1}{\alpha}} \Big[\int_0^t e^{-\beta s} \|e(s)\|^\beta ds \Big]^{\frac{1}{\beta}} \\ & + \frac{\varepsilon_0 ML}{\Gamma(\mu)} \left[\frac{e^{\alpha t}\Gamma\big(\alpha(\mu-1)+1\big)}{\alpha^{\alpha\mu-\alpha+1}} \right]^{\frac{1}{\alpha}} \bigg[\frac{(e^{\beta\tau_2}-1)\tau_4 e^{-\beta\tau_1}}{\beta} \|e(0)\|^\beta \\ & + \int_0^t \tau_4 e^{-\beta s} e^{-\beta\tau_1} \|e(s)\|^\beta ds \bigg]^{\frac{1}{\beta}} + \frac{(1-\varepsilon_0)ML}{\Gamma(\mu)} \left[\frac{e^{\alpha t}\Gamma\big(\alpha(\mu-1)+1\big)}{\alpha^{\alpha\mu-\alpha+1}} \right]^{\frac{1}{\alpha}} \\ & \times \bigg[\frac{(e^{\beta\tau_3}-1)\tau_4 e^{-\beta\tau_2}}{\beta} \|e(0)\|^\beta + \int_0^t \tau_4 e^{-\beta s} e^{-\beta\tau_2} \|e(s)\|^\beta ds \bigg]^{\frac{1}{\beta}} \bigg\} \\ \leqslant & \mathbb{E}\bigg\{ \bigg[1 + \frac{\varepsilon_0 MLe^t}{\Gamma(\mu)} \left(\frac{\Gamma\big(\alpha(\mu-1)+1\big)}{\alpha^{\alpha\mu-\alpha+1}} \right)^{\frac{1}{\alpha}} \left(\frac{(e^{\beta\tau_2}-1)\tau_4}{\beta} \right)^{\frac{1}{\beta}} e^{-\tau_1} \\ & + \frac{(1-\varepsilon_0)MLe^t}{\Gamma(\mu)} \left(\frac{\Gamma\big(\alpha(\mu-1)+1\big)}{\alpha^{\alpha\mu-\alpha+1}} \right)^{\frac{1}{\alpha}} \left(\frac{(e^{\beta\tau_3}-1)\tau_4}{\beta} \right)^{\frac{1}{\beta}} e^{-\tau_2} \bigg] \|e(0)\| \\ & + \bigg[\frac{(2M+ML)e^t}{\Gamma(\mu)} \left(\frac{\Gamma\big(\alpha(\mu-1)+1\big)}{\alpha^{\alpha\mu-\alpha+1}} \right)^{\frac{1}{\alpha}} + \frac{\varepsilon_0\tau_4 MLe^{t-\tau_1}}{\Gamma(\mu)} \\ & \times \left(\frac{\Gamma\big(\alpha(\mu-1)+1\big)}{\alpha^{\alpha\mu-\alpha+1}} \right)^{\frac{1}{\alpha}} + \frac{(1-\varepsilon_0)\tau_4 MLe^{t-\tau_2}}{\Gamma(\mu)} \left(\frac{\Gamma\big(\alpha(\mu-1)+1\big)}{\alpha^{\alpha\mu-\alpha+1}} \right)^{\frac{1}{\alpha}} \bigg] \\ & \times \int_0^t e^{-s} \|e(s)\| ds.\end{aligned} \tag{23}$$

An application of Lemma 2 yields that

$$
\begin{aligned}
\mathbb{E}\{\|e(t)\|\} \leqslant & \mathbb{E}\Bigg\{\Bigg[1+\frac{\varepsilon_0 MLe^t}{\Gamma(\mu)}\left(\frac{\Gamma(\alpha(\mu-1)+1)}{\alpha^{\alpha\mu-\alpha+1}}\right)^{\frac{1}{\alpha}}\left(\frac{(e^{\beta\tau_2}-1)\tau_4}{\beta}\right)^{\frac{1}{\beta}}e^{-\tau_1} \\
&+\frac{(1-\varepsilon_0)MLe^t}{\Gamma(\mu)}\left(\frac{\Gamma(\alpha(\mu-1)+1)}{\alpha^{\alpha\mu-\alpha+1}}\right)^{\frac{1}{\alpha}}\left(\frac{(e^{\beta\tau_3}-1)\tau_4}{\beta}\right)^{\frac{1}{\beta}}e^{-\tau_2}\Bigg]\|e(0)\| \\
&\times\Bigg[\frac{(2M+ML)e^t}{\Gamma(\mu)}\left(\frac{\Gamma(\alpha(\mu-1)+1)}{\alpha^{\alpha\mu-\alpha+1}}\right)^{\frac{1}{\alpha}}+\frac{\varepsilon_0\tau_4 MLe^{t-\tau_1}}{\Gamma(\mu)} \\
&\times\left(\frac{\Gamma(\alpha(\mu-1)+1)}{\alpha^{\alpha\mu-\alpha+1}}\right)^{\frac{1}{\alpha}}+\frac{(1-\varepsilon_0)\tau_4 MLe^{t-\tau_2}}{\Gamma(\mu)}\left(\frac{\Gamma(\alpha(\mu-1)+1)}{\alpha^{\alpha\mu-\alpha+1}}\right)^{\frac{1}{\alpha}}\Bigg] \\
&\times\exp\left(\int_0^t e^{-s}ds\right)\Bigg\} \\
=&\mathbb{E}\Bigg\{\Bigg[1+\frac{\varepsilon_0 MLe^t}{\Gamma(\mu)}\left(\frac{\Gamma(\alpha(\mu-1)+1)}{\alpha^{\alpha\mu-\alpha+1}}\right)^{\frac{1}{\alpha}}\left(\frac{(e^{\beta\tau_2}-1)\tau_4}{\beta}\right)^{\frac{1}{\beta}}e^{-\tau_1} \\
&+\frac{(1-\varepsilon_0)MLe^t}{\Gamma(\mu)}\left(\frac{\Gamma(\alpha(\mu-1)+1)}{\alpha^{\alpha\mu-\alpha+1}}\right)^{\frac{1}{\alpha}}\left(\frac{(e^{\beta\tau_3}-1)\tau_4}{\beta}\right)^{\frac{1}{\beta}}e^{-\tau_2}\Bigg]\|e(0)\| \\
&\times\Bigg[\frac{(2M+ML)e^t}{\Gamma(\mu)}\left(\frac{\Gamma(\alpha(\mu-1)+1)}{\alpha^{\alpha\mu-\alpha+1}}\right)^{\frac{1}{\alpha}}+\frac{\varepsilon_0\tau_4 MLe^{t-\tau_1}}{\Gamma(\mu)} \\
&\times\left(\frac{\Gamma(\alpha(\mu-1)+1)}{\alpha^{\alpha\mu-\alpha+1}}\right)^{\frac{1}{\alpha}}+\frac{(1-\varepsilon_0)\tau_4 MLe^{t-\tau_2}}{\Gamma(\mu)}\left(\frac{\Gamma(\alpha(\mu-1)+1)}{\alpha^{\alpha\mu-\alpha+1}}\right)^{\frac{1}{\alpha}}\Bigg] \\
&\times(1-e^{-t})\Bigg\} \\
=&\mathbb{E}\Big\{(1+\varepsilon_0 e^{t-\tau_1}H_1H_2+(1-\varepsilon_0)e^{t-\tau_2}H_1H_2)H_1M((2+L)e^t+\varepsilon_0\tau_4 Le^{t-\tau_1} \\
&+(1-\varepsilon_0)\tau_4 Le^{t-\tau_2})(1-e^{-t})\|e(0)\|\Big\}.
\end{aligned} \tag{24}
$$

From the condition given in (18), we have $\mathbb{E}\{\|e(t)\|\} \leqslant \gamma$. Thus, Systems (1) and (2) achieve QUS. □

Remark 5. *Different from the methods in [8,12,18,20,24–26,28,30], Hölder's inequality and Jensen's inequality are applied to explore QUS. Theorem 2 is not only related to the parameters of the system and expectation $\mathbb{E}$ but also related to the order of the system. Therefore, we can take different orders to compress, match and recognize the images in the applications of image processing.*

Remark 6. *In Theorems 1 and 2, the Lyapunov–Krasovskii functional approach and Volterra integral expansion are used to deduce the synchronization criteria, respectively, which is different from the usual way of dealing with probabilistic time-varying delay. In [17,21], the approaches to process probabilistic time-varying delay are applied by linear matrix inequalities (LMIs), where the obtained synchronization criteria are independent of the value of the derivative order. In this paper, Theorems 1 and 2 deeply reflect the influence of the order on the synchronization performance.*

4. Examples

Two illustrative examples are presented to further validate the theoretical results.

Example 1. *The two-state system given by (1) is considered, with* $\mu = 0.89$ *and activation functions* $y_1(v) = v + \frac{1}{6}|v|, y_2(v) = \tanh(v), \tau_1(t) = 0.2 + 0.2\cos(t), \tau_2(t) = 0.35 + 0.1\cos(t)$, $J = 0$,

$$A(t) = \begin{pmatrix} \frac{2}{1+t^2} & 0 \\ 0 & \frac{2}{1+t} \end{pmatrix}, \quad B(t) = \begin{pmatrix} 0.02\cos t & 0.5\sin t \\ 0.1\sin t & 0.3\cos t \end{pmatrix}, \quad C(t) = \begin{pmatrix} 0.1\sin t & 0.29\tanh t \\ 0.13\cos t & 0.22\sin t \end{pmatrix}.$$

According to the time-varying delay, we obtain $\theta_1 = -0.2, \theta_2 = 0.2, \theta_3 = -0.35$, $\theta_4 = 0.35$, $\tau_1 = 0.1, \tau_2 = 0.3$ and $\tau_3 = 0.4$. The constructed controller is

$$U_1(t) = -2.5e_1(t) + \frac{6.9e_1(t)}{\|e(t)\|^4 + 6.9^4}, \quad U_2(t) = -4e_2(t) + \frac{7.8e_2(t)}{\|e(t)\|^4 + 7.8^4}.$$

When $\varepsilon_0 = 0.6, l_1 = l_2 = 1, \theta_1 = 2.5$ and $\theta_2 = 1.5$, it is not difficult to confirm that $\Psi_1 = 3.97$, $\Psi_2 = 0.21$ and $\Psi_3 = 0.14$ satisfy the condition given in (9). Thus, Systems (1) and (2) can achieve QS under the order $\mu = 0.89$. The initial values are chosen as $v_{10} = -0.5$, $v_{20} = -3$, $v'_{10} = -2.5$ and $v'_{20} = 1.5$.

By MATLAB numerical simulations, Figures 1 and 2 characterize the trajectory curves of Systems (1) and (2) under the controller given in (8). Figure 3 presents the trajectory curves of the error system in (7). As can be seen from Figures 1 and 2, the trajectory curves of $v_i(t)$ and $v'_i(t)(i = 1,2)$ are not synchronized at the beginning (i.e., their trajectory curves do not coincide), subject to the initial values of the systems, the systems' parameters and the orders of the Caputo derivatives. However, the two trajectory curves gradually tend to coincide under the action of the controller given in (8), that is, they reach QS.

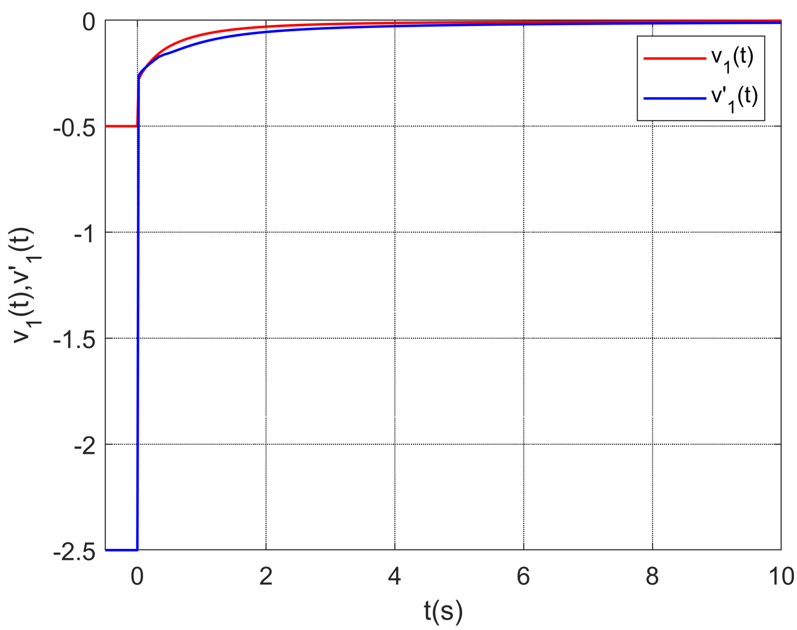

Figure 1. The trajectory lines of Systems (1) and (2) with $\mu = 0.89$ under the controller given in (8).

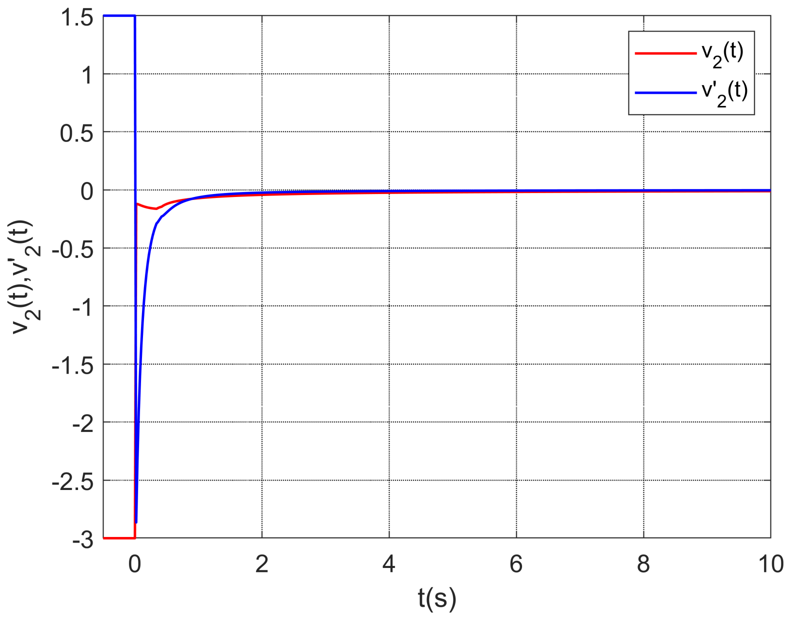

Figure 2. The trajectory lines of Systems (1) and (2) with $\mu = 0.89$ under the controller given in (8).

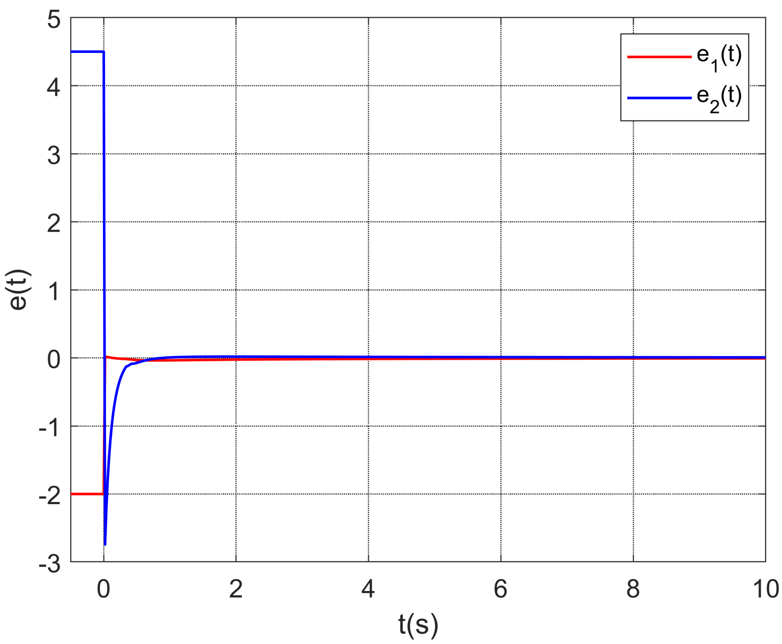

Figure 3. The trajectory lines of the error system in (3) with $\mu = 0.89$ under the controller given in (8).

Example 2. *The three-state fractional-order VPNN model (1) is considered, with* $\mu = 0.85$ *and activation functions* $y_1(v) = \tanh(v), y_2(v) = \cos(v), y_3(v) = \sin(v), J = 0$,

$$A(t) = \begin{pmatrix} \frac{2}{1+\sqrt{t}} & 0 & 0 \\ 0 & \frac{2}{1+t} & 0 \\ 0 & 0 & \frac{2}{1+t^2} \end{pmatrix}, \quad B(t) = \begin{pmatrix} 0.02\cos t & 0.5\sin t & 0.3\tanh t \\ 0.1\cos t & 0.4\sin t & 0.2\tanh t \\ 0.1\cos t & 0.25\sin t & 0.2\tanh t \end{pmatrix},$$

$$C(t) = \begin{pmatrix} \frac{1}{1+\sqrt{t}} & \frac{1}{1+t} & \frac{1}{1+t^2} \\ \frac{2}{1+\sqrt{t}} & \frac{2}{1+t} & \frac{2}{1+t^2} \\ \frac{3}{1+\sqrt{t}} & \frac{3}{1+t} & \frac{3}{1+t^2} \end{pmatrix}.$$

The time-varying delay is consistent with Example 1. Then, we can obtain $\theta_1 = -0.2$, $\theta_2 = 0.2, \theta_3 = -0.35, \theta_4 = 0.35, \tau_1 = 0.1, \tau_2 = 0.3$ and $\tau_3 = 0.4$. The constructed variable-parameter control gain is as follows:

$$\zeta(t) = \begin{pmatrix} \frac{1}{1+t} & 0 & 0 \\ 0 & \frac{1}{1+t^2} & 0 \\ 0 & 0 & \frac{1}{1+t^3} \end{pmatrix}.$$

Thus, we can calculate that $\tau_4 \approx 1.54$ and $M = 3$. If $\varepsilon_0 = 0.4, l_1 = l_2 = l_3 = 1, \alpha = \beta = 2$, $\delta = 0.03$ and $\gamma = 1$, then $\zeta(t), \beta(t)$ and $\sigma(t)$ satisfy the condition in (18). Namely, System (3) can achieve QUS. The QUS time is estimated as $T \approx 6.0882$. The initial values are chosen as $v_{10} = -0.5,\ v_{20} = -3,\ v_{30} = -2.5,\ v'_{10} = 2.5,\ v'_{20} = 1.5$ and $v'_{30} = 1.5$. By MATLAB numerical simulations, Figures 4–6 show the trajectory curves of System (7) under the controller given in (17). Similarly, the trajectory curves of $v_i(t)$ and $v'_i(t)(i = 1,2,3)$ are not synchronized at the beginning, from Figures 4–6. However, the trajectory curves gradually tend to coincide under the action of the controller given in (17), that is, they reach QUS. The controller can make the nodes in the NNs tend to be consistent from different states so that whole NNs will reach a synchronized state. Figure 7 characterizes the trajectory curves of the error system in (7). Therefore, Systems (1) and (2) can achieve QUS under the order $\mu = 0.85$.

Remark 7. *Inspired by the simulation method in [34,35], we improve the predictor-corrector scheme of fractional delayed differential equations to verify the effectiveness and correctness of the theoretical results. The predictor-corrector scheme provides the predicted value by the iteration step by step based on the initial value and an explicit formula, and then the correction value is obtained by an implicit formula. That is, the fractional delayed differential equation is expressed as the Volterra integral equation, and Adams–Bashforth predictor and corrector values are obtained on the basis of selecting the appropriate step length. Finally, numerical simulations are performed based on the corresponding error estimation and MATLAB toolbox.*

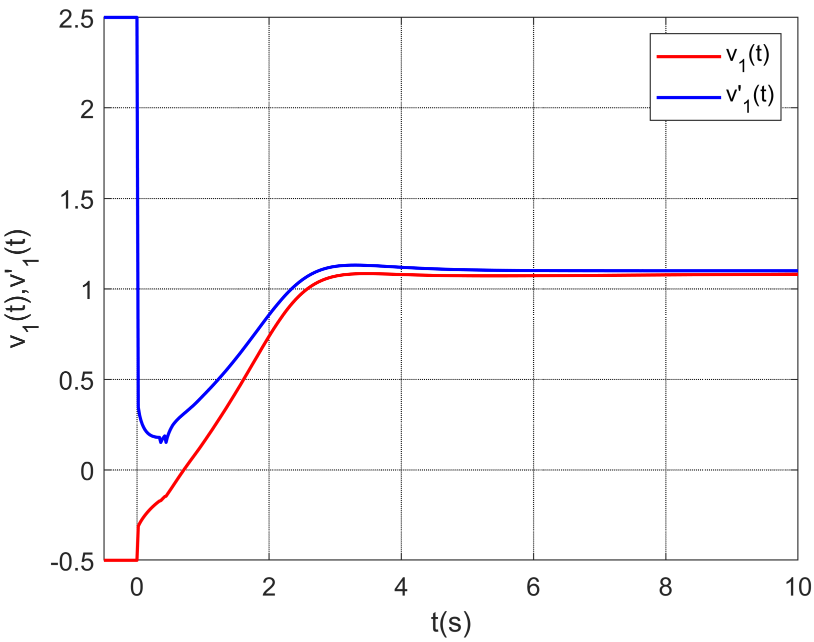

Figure 4. The trajectory lines of Systems (1) and (2) with $\mu = 0.85$ under the controller given in (17).

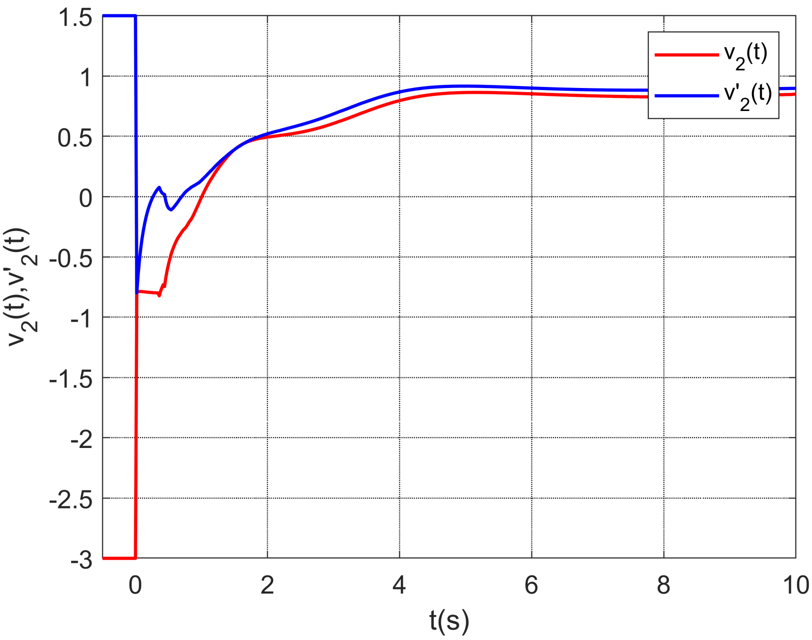

Figure 5. The trajectory lines of Systems (1) and (2) with $\mu = 0.85$ under the controller given in (17).

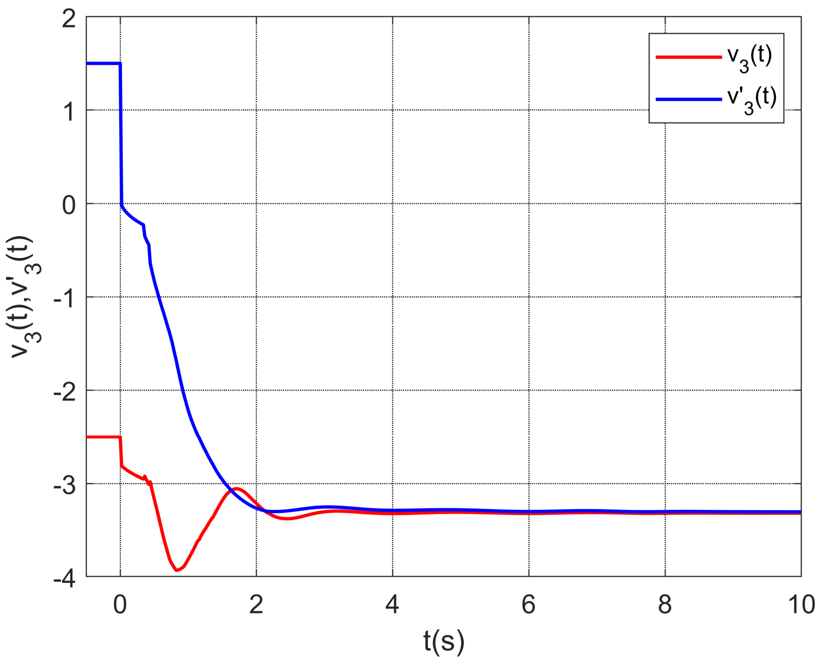

Figure 6. The trajectory lines of Systems (1) and (2) with $\mu = 0.85$ under the controller given in (17).

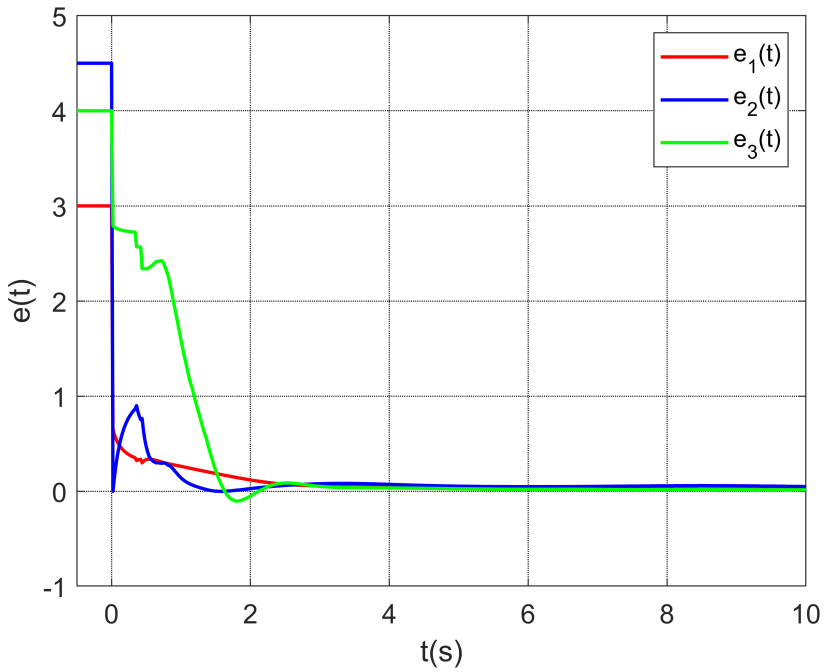

Figure 7. The trajectory lines of the error system in (3) with $\mu = 0.85$ under the controller given in (17).

5. Discussions

In this paper, we consider the effects of the system parameters, the probability distributions and the order of Caputo derivative on QS and QUS. Different from the methods in [8,12,18,20,24–26,28,30], Hölder's inequality and Jensen's inequality are applied to explore the QS and QUS.

Theorems 1 and 2 are related to the probability distributions and the order of the Caputo derivative, which deeply reveals the factors affecting synchronization performance.

In the field of solving nonlinear fractional ordinary differential equations, there are not as many numerical algorithms as there are in integer-order ordinary differential equations. Only a limited number of common methods have been translated to the fractional domain, such as the predictor-corrector path based on Adams–Bashforth–Moulton [34,35]. The synchronization test of drive–response systems by the improved Adams–Bashforth–Moulton predictor-corrector way is presented in this paper. By MATLAB numerical simulations, Figures 1–7 show the trajectory curves of System (7) under the controllers given in (8) or (17), which are consistent with Theorems 1 and 2.

6. Conclusions

This paper has focused on investigating the QS and QUS between drive–response systems for fractional-order VPNNs (1) with probabilistic time-varying delays. We have simultaneously taken into account the effects of the system parameters, the probability distributions and the Caputo order on QS and QUS. By applying the Lyapunov functional approach, Hölder's inequality and Jensen's inequality, Theorems 1 and 2 under controller designs with the constant gain coefficient in (8) and the time-varying gain coefficient in (17) have been established. The method and results of this paper can greatly reduce calculation complexities. Under different probability distributions, two numerical simulation examples have demonstrated the feasibility of Theorems 1 and 2. In the future, the dynamics of fractional-order VPNNs with probabilistic time-varying delays in the complex field and quaternion-valued field will be further explored.

Author Contributions: R.Y.: writing—original draft, methodology. C.W.: writing—review and editing, software. A.S.: conceptualization, validation. H.Z.: methodology, supervision. All authors have read and agreed to the published version of the manuscript.

Funding: This work was supported by the Natural Science Foundation of Anhui Province of China (No. 1908085MA01) and the Natural Science Foundation of the Higher Education Institutions of Anhui Province of China (KJ2019A0557, KJ2020A0503).

Institutional Review Board Statement: Not applicable.

Informed Consent Statement: Not applicable.

Data Availability Statement: Not applicable.

Conflicts of Interest: The authors declare that they have no competing interest.

References

1. Nardo, F.; Morbidoni, C.; Cucchiarelli, A.; Fioretti, S. Influence of EMG-signal processing and experimental set-up on prediction of gait events by neural network. *Biomed. Signal Process Control* **2021**, *63*, 102232. [CrossRef]
2. Alapuranen, P.; Schroeder, J. Complex artificial neural network with applications to wireless communications. *Digit. Signal Process.* **2021**, *119*, 103194. [CrossRef]
3. Karasu, S.; Altan, A. Crude oil time series prediction model based on LSTM network with chaotic Henry gas solubility optimization. *Energy* **2022**, *242*, 122964. [CrossRef]
4. Stamova, I.; Sotirov, S.; Sotirova, E.; Stamov, G. Impulsive fractional Cohen-Grossberg neural networks: almost periodicity analysis. *Fractal Fract.* **2021**, *5*, 78. [CrossRef]
5. Thakur, N.; Han, C. A study of fall detection in assisted living: identifying and improving the optimal machine learning method. *J. Sens. Actuator Netw.* **2021**, *10*, 39. [CrossRef]
6. Arena, P.; Caponetto, R.; Fortuna, L.; Porto, D. Bifurcation and chaos in noninteger order cellular neural networks. *Int. J. Bifurcat. Chaos* **1998**, *8*, 1527–1539. [CrossRef]
7. Song, Q.; Chen, Y.; Zhao, Z.; Liu, Y. Robust stability of fractional-order quaternion-valued neural networks with neutral delays and parameter uncertainties. *Neurocomputing* **2021**, *420*, 70–81. [CrossRef]
8. Wang, C.; Zhang, H.; Zhang, H.M.; Zhang, W. Globally projective synchronization for Caputo fractional quaternion-valued neural networks with discrete and distributed delays. *AIMS Math.* **2021**, *6*, 14000–14012. [CrossRef]
9. Arslan, E.; Narayanan, G.; Ali, M.; Arik, S.; Saroha, S. Controller design for finite-time and fixed-time stabilization of fractional-order memristive complex-valued BAM neural networks with uncertain parameters and time-varying delays. *Neural Netw.* **2020**, *130*, 60–74. [CrossRef]
10. Aravind, R.; Balasubramaniam, P. Global asymptotic stability of delayed fractional-order complex-valued fuzzy cellular neural networks with impulsive disturbances. *J. Appl. Math. Comput.* **2022**. [CrossRef]
11. Agarwal, R.; Hristova, S.; O'Regan, D. Global Mittag-Leffler synchronization for neural networks modeled by impulsive Caputo fractional differential equations with distributed delays. *Symmetry* **2018**, *10*, 473. [CrossRef]
12. Ali, M.; Hymavathi, M.; Senan, S.; Shekher, V.; Arik, S. Global asymptotic synchronization of impulsive fractional-order complex-valued memristor-based neural networks with time varying delays. *Commun. Nonlinear Sci. Numer. Simul.* **2019**, *78*, 104869. [CrossRef]
13. Wang, Z.; Cao, J.; Cai, Z.; Tan, X.; Chen, R. Finite-time synchronization of reaction-diffusion neural networks with time-varying parameters and discontinuous activations. *Neurocomputing* **2021**, *447*, 272–281. [CrossRef]
14. Cheng, Y.; Zhang, H.; Zhang, W.; Zhang, H.M. Novel algebraic criteria on global Mittag-Leffler synchronization for FOINNs with the Caputo derivative and delay. *J. Appl. Math. Comput.* **2021**, 211. [CrossRef]
15. Pratap, A.; Raja, R.; Cao, J.; Rajchakit, G.; Alsaadi, F. Further synchronization in finite time analysis for time-varying delayed fractional order memristive competitive neural networks with leakage delay. *Neurocomputing* **2018**, *317*, 110–126. [CrossRef]
16. Gu, Y.; Yu, Y.; Wang, H. Projective synchronization for fractional-order memristor-based neural networks with time delays. *Neural Comput. Appl.* **2019**, *31*, 6039–6054. [CrossRef]
17. Chen, S.; Song, Q.; Zhao, Z.; Liu, Y.; Alsaadi, F.E. Global asymptotic stability of fractional-order complex-valued neural networks with probabilistic time-varying delays. *Neurocomputing* **2021**, *450*, 311–318. [CrossRef]
18. Zhang, W.; Zhang, H.; Cao, J.; Alsaadi, F.; Chen, D. Synchronization in uncertain fractional-order memristive complex-valued neural networks with multiple time delays. *Neural Netw.* **2019**, *110*, 186–198. [CrossRef]
19. Cao, J.; Stamova, G.; Stamova, I.; Simeonov, S. Almost periodicity in impulsive fractional-order reaction-diffusion neural networks with time-varying delays. *IEEE Trans. Cybern.* **2021**, *51*, 151–161. [CrossRef]
20. Zhang, H.; Ye, M.; Ye, R.; Cao, J. Synchronization stability of Riemann-Liouville fractional delay-coupled complex neural networks. *Phys. A* **2018**, *508*, 155–165. [CrossRef]
21. Lakshmanan, S.; Park, J.; Lee, T.; Jiang, H.; Rakkiyappan, R. Stability criteria for BAM neural networks with leakage delays and probabilistic time-varying delays. *Appl. Math. Comput.* **2013**, *219*, 9408–9423. [CrossRef]

22. Yang, J.P.; Li, H.; Yang, J.K.; Zhang, L.; Jiang, H. Quasi-synchronization and complete synchronization of fractional-Order fuzzy BAM neural networks via nonlinear control. *Neural Process. Lett.* **2022**, 176. [CrossRef]
23. Zahra, A.; Biswadip, D.; Elizabeth, N.; Naomi, E. Cluster synchronization of diffusively-coupled nonlinear systems: A contraction based approach. *J. Nonlinear Sci.* **2020**, *30*, 2235–2257. [CrossRef]
24. Zhang, W.; Sha, C.; Cao, J.; Wang, G.; Wang, Y. Adaptive quaternion projective synchronization of fractional order delayed neural networks in quaternion field. *Appl. Math. Comput.* **2021**, *400*, 126045. [CrossRef]
25. Liu, P.; Kong, M.; Zeng, Z. Projective synchronization analysis of fractional-order neural networks with mixed time delays. *IEEE Trans. Cybern.* **2021**, *400*, 1–11. [CrossRef]
26. Zhang, W.; Cao, J.; Wu, R.; Chen, D.; Alsaadi, F. Novel results on projective synchronization of fractional-order neuraln networks with multiple time delays. *Chaos Solitons Fractals* **2018**, *117*, 76–83. [CrossRef]
27. Zhang, L.; Yang, Y.; Wang, F. Lag synchronization for fractional-order memristive neural networks via period intermittent control. *Nonlinear Dyn.* **2017**, *89*, 367–381. [CrossRef]
28. Ye, R.; Liu, X.; Zhang, H.; Cao, J. Global Mittag-Leffler synchronization for fractional-order BAM neural networks with impulses and multiple variable delays via delayed-feedback control strategy. *Neural Process. Lett.* **2019**, *49*, 1–18. [CrossRef]
29. Zhang, H.; Cheng, Y.; Zhang, H.M.; Zhang, W.; Cao, J. Hybrid control design for Mittag-Leffler projective synchronization on FOQVNNs with multiple mixed delays and impulsive effects. *Math. Comput. Simul.* **2022**, *197*, 341–357. [CrossRef]
30. Xiao, J.; Cao, J.; Cheng, J.; Zhong, S.; Wen, S. Novel methods to finite-time Mittag-Leffler synchronization problem of fractional-order quaternion-valued neural networks. *Inf. Sci.* **2020**, *526*, 221–244. [CrossRef]
31. Zheng, M.; Li, L.; Peng, H.; Xiao, J.; Yang, Y.; Zhang, Y.; Zhao, H. Finite-time stability and synchronization of memristor-based fractional-order fuzzy cellular neural networks. *Commun. Nonlinear Sci. Numer Simul.* **2018**, *59*, 272–291. [CrossRef]
32. Wu, H.; Zhang, X.; Xue, S.; Niu, P. Quasi-uniform stability of Caputo-type fractional-order neural networks with mixed delay. *Int. J. Mach. Learn. Cybern.* **2017**, *8*, 1501–1511. [CrossRef]
33. Zhang, H.; Cheng, J.; Zhang, H.M.; Zhang, W.; Cao, J. Quasi-uniform synchronization of Caputo type fractional neural networks with leakage and discrete delays. *Chaos Solitons Frac.* **2021**, *152*, 111432. [CrossRef]
34. Diethelm, K. An efficient parallel algorithm for the numerical solution of fractional differential equations. *Fract. Calc. Appl. Anal.* **2011**, *14*, 475–490. [CrossRef]
35. Odibat, Z.; Baleanu, D. Numerical simulation of initial value problems with generalized Caputo-type fractional derivatives. *Appl. Numer. Math.* **2020**, *156*, 94–105. [CrossRef]
36. Podlubny, I. *Fractional Differential Equations*; Academic Press: New York, NY, USA, 1999.